A reassessment of lake and wetland feedbacks on the North African Holocene climate

Gerhard Krinner, Anne-Marie Lézine, Pascale Braconnot, Pierre Sepulchre, Gilles Ramstein, Christophe Grenier, I. Gouttevin

A reassessment of lake and wetland feedbacks on the North African Holocene climate

G. Krinner,[1] A.-M. Lézine,[2] P. Braconnot,[2] P. Sepulchre,[2] G. Ramstein,[2] C. Grenier,[2] and I. Gouttevin[1,3]

Received 24 January 2012; revised 2 March 2012; accepted 2 March 2012; published 3 April 2012.

[1] Large parts of the Sahara were vegetated during the early to mid Holocene. Several positive feedbacks, most notably related to vegetation, have been shown to have favored the northward migration of the desert boundary. During this period, numerous lakes and wetlands existed in the Sahara region and might have acted as a local moisture source. However, earlier model studies of the effects of open water surfaces on the mid-Holocene North African climate suggested that these were weak and did not contribute significantly to this northward migration of the North African climate zones. Using a state-of-the-art climate model, we suggest that the effect of open-water surfaces on the mid-Holocene North African climate might have been much stronger than previously estimated, regionally more than doubling the simulated precipitation rates. It is thus possible that this effect, combined to other known positive feedbacks, favored the appearance of the "Green Sahara".
Citation: Krinner, G., A.-M. Lézine, P. Braconnot, P. Sepulchre, G. Ramstein, C. Grenier, and I. Gouttevin (2012), A reassessment of lake and wetland feedbacks on the North African Holocene climate, *Geophys. Res. Lett.*, *39*, L07701, doi:10.1029/2012GL050992.

1. Introduction

[2] During the early to mid-Holocene African humid period, parts of the now hyper-arid Sahara were vegetated [*Ritchie et al.*, 1985; *Hoelzmann et al.*, 1998; *Prentice and Jolly, 2000*; *Watrin et al.*, 2009] and inhabited [*Kuper and Kröpelin*, 2006]. Inland water surfaces, now mostly desiccated, were widespread [*Street and Grove*, 1976; *Hoelzmann et al.*, 1998; *Kröpelin et al.*, 2008; *Gasse*, 2000; *Lézine et al.*, 2011].

[3] This humid period was certainly triggered by orbital forcing [*Kutzbach*, 1981; *Rossignol-Strick*, 1983], but it has been shown that positive feedbacks within the Earth system have operated to amplify this forcing in order to obtain a "Green Sahara" [e.g., *Braconnot et al.*, 2007]. *Kutzbach and Liu* [1997] and *Braconnot et al.* [1999] identified oceanic feedbacks that amplified this orbital forcing, while *Kutzbach et al.* [1996] and *Claussen et al.* [1999] showed that an increased vegetation cover could amplify the orbital forcing through intensified precipitation recycling and the vegetation albedo feedback. In this context, *Bonfils et al.* [2001] showed that simulated mid-Holocene precipitation change (compared to present and in the absence of calculated vegetation changes) is stronger if the prescribed background bare soil albedo in a climate model is lower. This is clearly in line with the analysis by *Charney* [1975] who suggested that an increased surface albedo suppresses atmospheric ascendance and, thus, leads to reduced precipitation rates. This effect is illustrated in more recent work by *Knorr and Schnitzler* [2006] and *Vamborg et al.* [2011] who show that the orbitally triggered mid-Holocene Sahel precipitation increase can be amplified in a climate model if a soil albedo scheme is used that takes into account simulated or prescribed vegetation cover and litter.

[4] Concerning open water surfaces, *Coe and Bonan* [1997] showed that open water surfaces provide a further positive feedback amplifying the Holocene orbital forcing. Prescribing open water surfaces in line with reconstructed mid-Holocene surface water extent in a climate model led to a significant strengthening of the simulated monsoon circulation and increased precipitation south of 20°N, but not further north. Using the same general circulation model, *Broström et al.* [1998] performed some additional numerical experiments of the effect of lakes and wetlands. In their simulations, unlike in the work by *Coe and Bonan* [1997], a reconstructed mid-Holocene vegetation distribution was prescribed. However, similar to *Coe and Bonan* [1997], their simulations did not yield any further northward penetration of the monsoon rain caused by the presence of open-water surfaces, compared to simulations without lakes and wetlands.

[5] It is debated whether the transition between the Holocene "Green Sahara" to the modern hyperarid desert at the end of the African humid period was abrupt, as *deMenocal et al.* [2000] suggested after evidence of an abrupt onset of windblown dust in oceanic sediment cores taken off the coast of the Western Sahara, or whether this transition was more gradual, as *Kröpelin et al.* [2008] suggested based on an analysis of vegetation changes in Sahara lake sediments, or whether the type of the transition differed between the eastern and western part of the Sahara [*Brovkin and Claussen*, 2008]. An abrupt transition to dry conditions as a response to gradually changing orbital forcing would point to efficient positive feedbacks, while a more gradual response could indicate that positive feedbacks favoring the establishment of "green Sahara" conditions could partially be muted at the end of a humid period. Concerning this question, a coupled transient simulation of the evolution of the northern Africa climate-ecosystem for the last 6500 years [*Liu et al.*, 2007] suggested concurrent gradual precipitation and more abrupt vegetation changes at the end of the African humid period. *Liu et al.* [2007] concluded that the possibly abrupt vegetation collapse was not induced by a strong positive vegetation feedback, but rather by low-frequency climate variability [*Liu et al.*, 2006]. However, this view has been challenged by *Bathiany et al.* [2012] whose modelling study suggested that the vegetation collapse could

[1]CNRS/Université Joseph Fourier–Grenoble 1, LGGE, Grenoble, France.
[2]LSCE/IPSL, CEA/CNRS/UVSQ, Gif sur Yvette, France.
[3]AgroParisTech, ENGREF, Paris, France.

0094-8276/12/2012GL050992

have arisen because of a strong atmosphere-vegetation feedback combined with an impact of the vegetation cover on the amplitude of temporal variability in the system.

[6] Although more and more land-surface feedbacks are represented in current-generation climate models, simulating a mid-Holocene North African climate in line with evidence from paleoclimatic data remains a challenge for many models. Therefore, it is possible that one or several positive feedbacks for rainfall over the region are missing in some of these models. It is necessary to identify these feedbacks in order to realistically simulate the North African Holocene climate and to help clarify the issue of abrupt or gradual transition between humid and arid periods over the Sahara. More than 10 years after pioneering study by *Coe and Bonan* [1997] and the additional analysis by *Broström et al.* [1998], the present study provides a reassessment of the effect of prescribed open-water surfaces in the context of the Saharan mid-Holocene climate, taking into account potential feedbacks linked to vegetation and soil albedo changes.

2. Methods

[7] In order to evaluate the effect of open-water surfaces, we used a version of the LMDZ atmospheric general circulation model (AGCM) [*Hourdin et al.*, 2006] which includes a module representing the climatologically relevant thermal and hydrological processes occurring above and beneath inland water surfaces [*Krinner*, 2003]. Because the strong feedback between vegetation and precipitation in the Sahara region [*Claussen and Gayler*, 1997] could substantially modify the effect of open water surfaces on precipitation amount, the AGCM is asynchronously coupled to the BIOME4 equilibrium vegetation model [*Kaplan et al.*, 2003] for the paleoclimate simulations. Depending on the prescribed biogeography, the land surface module used in LMDZ [*Krinner et al.*, 2005] specifies the vegetation properties relevant for surface-atmosphere exchanges of energy, momentum and water such as surface roughness, LAI etc. In addition, where the simulated annual maximum vegetation fraction (more precisely, foliage projected cover) exceeds 20%, the prescribed mid-Holocene soil type is modified such as to replace the modern high desert soil albedo (0.27) by darker soils (with an albedo between 0.16 and 0.18, depending on soil humidity).

[8] The model version used here has 19 vertical layers and was run at a regional resolution of 1 degree (110 km) in latitude and 1.5 degrees (∼140 km at 30°N) in longitude over the Sahara. The resolution of this global model slowly degrades outside of the region of interest. A 21-year control simulation for present-day climatic conditions was forced by appropriate average 1980–2000 HADISST sea surface conditions [*Rayner et al.*, 2003], greenhouse gas concentrations, orbital configuration, vegetation distribution and inland water surface fractions. In addition, two 9-kyr BP and two 6-kyr BP simulations were carried out. Each paleoclimate simulation uses appropriate greenhouse gas concentrations [*Flückiger et al.*, 2002], orbital parameters [*Berger*, 1978], and sea-surface condition anomalies. These sea-surface condition anomalies are taken from IPSL-CM4 coupled ocean-atmosphere general circulation model simulations for 9 and 6 kyr BP [*Marzin and Braconnot*, 2009] and added to the present-day sea-surface conditions.

[9] Groundwater inflow into the open water surfaces, a process still maintaining sporadic lakes in the Sahara although the last significant recharge of the aquifer systems occurred during the late Holocene [*Gasse*, 2000], is represented by imposing a minimum depth of 0.2 m in wetlands and 1 m in lakes.

[10] One simulation for each paleoclimatic period (referred to as C9L6 and C6L6 in the following) uses reconstructed 6 kyr BP North African inland water surface fractions [*Hoelzmann et al.*, 1998] occupying 7.6% of the North African land surface between 10°N and 30°N at 6 kyr BP. The other simulation (C9L0 and C6L0, respectively) is run with present-day inland water surfaces, which occupy at present about 0.5% of the land surface in this area [*Cogley*, 2003]. Starting from a reconstructed 6 kyr BP initial vegetation distribution [*Hoelzmann et al.*, 1998], two iterations of the coupled model system are carried out by first running the AGCM for several decades, using its stabilized output to compute a new equilibrium vegetation distribution with BIOME4, and feeding back this new vegetation distribution and the corresponding soil albedo changes into the AGCM. The differences between the first and the second computed vegetation distribution are marginal. A final 42-year simulation, using the second computed vegetation distribution, is then carried out with the AGCM. The last 41 years of this run are used for the analysis presented here.

[11] To diagnose drought frequencies, we use the drought area index method defined by *Bhalme and Mooley* [1980]. For each month k, the drought area index I_k is recursively calculated as: $I_k = a\, I_{k-1} + b\, (p_k - q_k)/\sigma_k$, where I_k is the previous month's drought index, p_k is the precipitation of month k, q_k is the multiannual mean precipitation of that month, σ_k is the interannual precipitation variability of that month, and the two parameters $a = 0.51$ and $b = 0.0206$ [*Keyantash and Dracup*, 2002]. By construction, negative values of I indicate prolonged drier-than-average conditions.

3. Results

[12] Most of the following analysis concentrates on the situation at 9 kyr BP, because the results and in particular the climatic impact of the open water surfaces are very similar at 9 and 6 kyr BP.

[13] The zonal average simulated precipitation amount over continental Africa (Figure 1) is in good agreement with recent climatologies [*Hulme et al.*, 1998; *Hijmans et al.*, 2005] except for an overestimate in the equatorial belt. The impact of the open water surfaces on the simulated North African mid-Holocene precipitation is positive over all latitude bands. It leads to a ∼1.5 degree (∼160 km) northward shift of the isohyets in the Sahel and the southern Sahara (Figure 1). The relative precipitation increase is particularly strong, in excess of 50%, in the central and western Sahara where annual mean precipitation rates are about 250 mm/yr (Figures 2a and 2b), while it is weaker in the wetter area further south. The obvious reason for this is that in a relatively dry background climate, a given amount of evaporation from open water surfaces will represent a larger fraction of the precipitable water in the atmosphere. The Sahara north of ≈25°N is somewhat dryer at 9 kyr than at 6 kyr BP (not shown), contrary to the more southerly regions which are dryer at 6 kyr than at 9 kyr BP in the no-lake simulations, as a consequence of the more intense 9 kyr BP monsoon caused by stronger summer insolation [*Marzin and Braconnot*, 2009]. Indeed, the annual precipitation maximum in the western Sahara (around 25°N) occurs in August in most of our simulations, and insolation differences

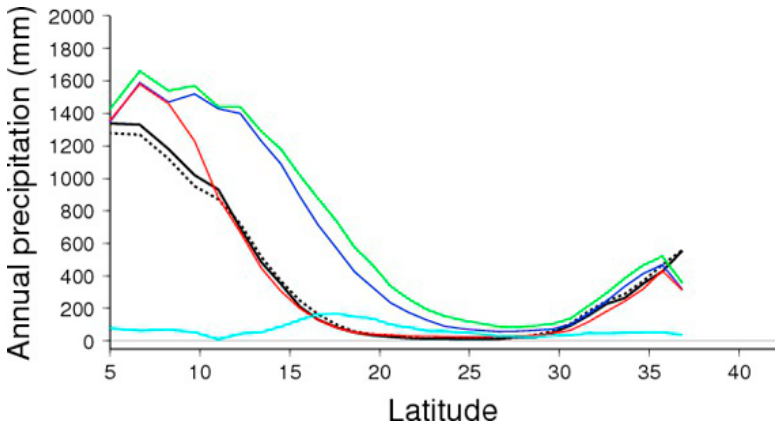

Figure 1. Annual average zonal mean precipitation over Africa. Observed (full black: WorldClim [*Hijmans et al.*, 2005]; dotted black: Climate Research Unit [*Hulme et al.*, 1998]) annual mean zonal mean precipitation over continental Africa for the present, in mm/yr; simulated precipitation (mm/yr) for the present-day reference simulation (red), C9L0 (blue) and C9L6 (green); and difference between C9L6 and C9L0 (turquoise).

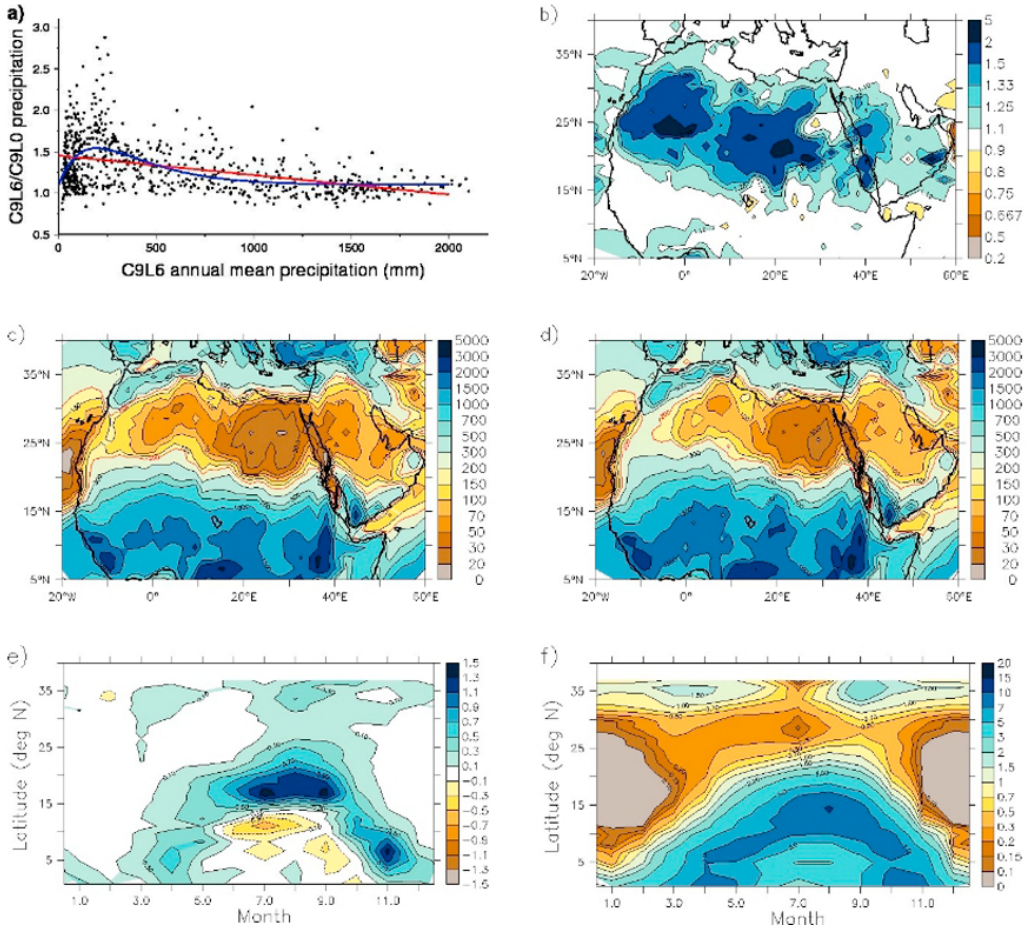

Figure 2. Holocene annual mean precipitation and impact of open water surfaces. (a) Ratio between C9L6 and C9L0 annual mean precipitation as a function of C9L6 annual mean precipitation for North African land grid points from 10°N to 40°N and from 20°W to 60°E; red line: linear RMSE fit of type $y = a + bx$; blue line: 3-parameter RMSE fit of type $y = a + bxe^{-cx}$. (b) Ratio between C9L6 and C9L0 annual mean precipitation, that is, relative effect of the open water surfaces (dimensionless). (c) C9L0 annual mean precipitation (mm/year, 200 mm/yr isohyet in red). (d) C9L6 annual mean precipitation (mm/year, 200 mm/yr isohyet in red). (e) Precipitation rate difference between C9L6 and C9L0 (mm/day) as a function of month and latitude, averaged for North African land grid points from 20°W to 60°E. (f) Precipitation rate of C9L6 (mm/day) as a function of month and latitude, averaged for North African land grid points from 20°W to 60°E.

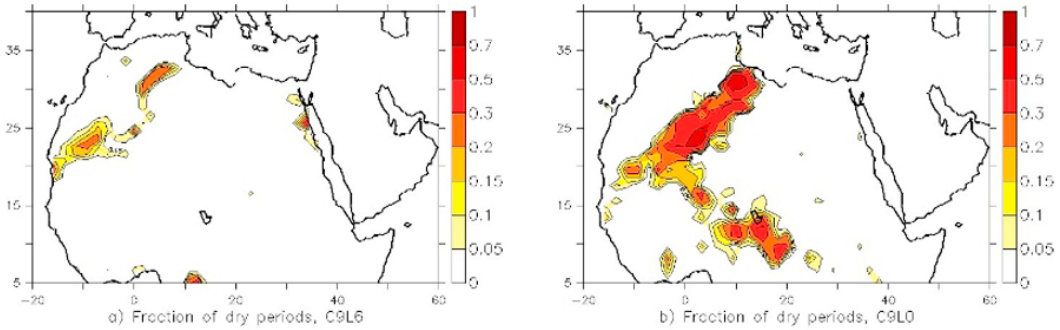

Figure 3. Simulated drought frequency: (a) C9L6 and (b) C9L0. Temporal fraction of drought (defined as drought area index $I < -0.5$). Unit: dimensionless (between 0 and 1).

between 9 and 6 kyr BP at this latitude are very small during that month [*Marzin and Braconnot*, 2009]. Therefore higher precipitation rates at 9 kyr BP than at 6 kyr BP are not to be expected in this region. Moreover, this is consistent with a recent compilation [*Lézine et al.*, 2011] which shows that the North African wetland extent reached its maximum at about 6 kyr BP.

[14] The additional precipitation induced by the open water surfaces leads to a substantial eastward retreat of the isohyets in the central Sahara (Figures 2c and 2d), creating a continuous meridional band of annual mean precipitation in excess of 200 mm/yr across the western Sahara. Because the 200 mm/yr isohyet corresponds well to the transition between desert and xerophytic shrubland as simulated by Biome4 in North Africa for early and mid-Holocene conditions, this is equivalent to a continuous band of vegetation. The regional west-east gradient of Holocene precipitation, and the associated preferential development of vegetation in the western Sahara, is a feature supported by paleoecological data [*Pachur and Hoelzmann*, 2000; *Ritchie and Haynes*, 1987; *Lézine*, 1989]. Given that the simulations presented here focus on the latter part of the African humid period, it is consistent with reconstructions of the spatiotemporal dynamics of inland water surface occurrence [*Lézine et al.*, 2011] which suggests both an earlier wettening and an earlier desiccation in the Eastern Sahara than in its western part.

[15] The relative precipitation increase in the central Sahara is rather evenly distributed throughout the year. Consequently the absolute precipitation change induced by the inland water surfaces (Figure 2e) has a similar spatiotemporal monsoon-type structure as the precipitation itself (Figure 2f), that is, it is maximum in summer. This intensification of the monsoon circulation leads to a slightly more northerly intrusion of monsoon precipitation into North Africa during the second half of the year. As a consequence, the partitioning between convective and large-scale precipitation shifts to more convective precipitation in the central Sahara. South of the desert/shrubland ecotone, however, an opposite shift of the partitioning between convective and large-scale precipitation occurs. It is associated with a summer surface cooling ($\sim -1^{\circ}$C) linked to the increased evaporation rates from both vegetation and inland water surfaces. Over most of Northern Africa, larger thermal inertia of the open water surfaces delays cooling during the boreal autumn and thus slightly delays the end of the monsoon season. However, the high thermal inertia of deeper lakes can also locally suppress precipitation, as can be seen over the Mega-Lake Chad (Figure 2b): the relatively cool surface of this extremely large lake stabilizes the atmosphere and thus reduces convective precipitation. The evaporative effect of the open water surfaces (a local moisture source leading to precipitation recycling) nevertheless dominates their thermal effect (stabilization of the vertical atmospheric structure) on the continental scale because grid-scale surface temperature is dominated by the normal continental surface due to the generally fairly small horizontal extent of open-water surfaces [*Hoelzmann et al.*, 1998].

[16] During humid periods, the negative surface mass balance of the open water surfaces (of about -4 mm/day in our simulations) must be compensated for by groundwater inflow [*Gasse*, 2000] as a consequence of water-table rise in the aquifers, or surface runoff from adjacent land. The more positive hydrological balance on the southern fringe of the Sahara appears correctly simulated by our model, because the simulated evaporative loss over the surface of Lake Chad, with its prescribed extent equal to the reconstructed $\sim$340,000 km^2 Holocene maximum [*Leblanc et al.*, 2006], is overcompensated for by precipitation over the lake and runoff from within the hydrological basin of Lake Chad.

[17] Over the Western Sahara, the presence of inland water surfaces drastically reduces the drought occurrence (Figure 3), here defined as the fraction of months during which the drought area index is below -0.5 (negative numbers indicating drier than average conditions). More specifically, in the areas with annual mean precipitation between 200 and 300 mm, which are close to the transition from xerophytic shrubland to desert and which are the areas where the precipitation increase due to inland water surfaces tends to be strongest (Figure 2a), the spatial average temporal fraction of drought conditions is 2.4% in C9L6 and 7.2% in C9L0. This means that for the same given amount of annual mean precipitation, drought conditions are much less frequent in the presence of inland water surfaces. Concurrently, the spatial average of the lowest drought area index decile in these areas is -0.30 in C9L6 and -0.36 in C9L0, indicating less severe droughts for similar mean climatic conditions when inland water surfaces are present.

4. Discussion

[18] At the end of the African humid period, ecosystem changes were induced by insolation [*Rossignol-Strick*, 1983] and internal positive feedbacks through vegetation [*Claussen and Gayler*, 1997] and oceanic circulation changes [*Kutzbach*

and Liu, 1997; *Braconnot et al.*, 1999]. Our model results, combined with the almost total absence of open water surfaces in the Sahara today, indicate that the changes were reinforced by a positive feedback loop linked to open-water surfaces. Reduced precipitation over North Africa led to reduced open water surfaces, which in turn reduced precipitation rates. However, this positive feedback was not necessarily immediate. A significant delay between the onset of more arid climate conditions and the final desiccation of the Saharan lowlands is probable because the rate of drawdown of the Sahara-Sahel groundwater reservoirs, which fed the open water surfaces by seepage [*Gasse*, 2002], is typically very low [*Gasse*, 2000]. Fossil groundwater still feeds residual lakes such as Lake Yoa [*Kröpelin et al.*, 2008] and is generally fairly close to the ground surface in depression areas above the Nubian Sandstone Aquifer System [*Kröpelin et al.*, 2008 ; *Gasse*, 2002], about 7000 years after the last recharge period. The end of the African humid period, a reaction of the coupled regional climate system to the orbital forcing, could therefore have been delayed or temporally smoothed by the open water surfaces: these continued to be fed by groundwater inflow for typically about 1000 years (C. Grenier et al., Hydrological reconstruction of the Ounianga lake redion (NE Chad) during the Holocene period, submitted to *Journal of Hydrology*, 2012) and buffered the rapid positive vegetation feedback by providing a source of atmospheric moisture on the local and regional scales. This allows to reconcile our understanding of the dynamics of the Saharan climate system with recent findings [*Kröpelin et al.*, 2008] which suggest that the drying of the Eastern Sahara was more gradual than previously thought on the basis of observations of a sudden onset of dust deflation in the western Sahara at about 5500 BP [*deMenocal et al.*, 2000].

[19] *Coe and Bonan* [1997] and *Broström et al.* [1998] have previously reported a precipitation increase in mid-Holocene North Africa as a consequence of imposed open-water surfaces. However, in these older articles reporting on simulations carried out with the CCM3 climate model, the reported precipitation increase is much weaker than the increase shown here and, importantly, essentially vanishes northwards of about 20°N. Therefore, *Broström et al.* [1998] do not simulate a significant retreat of the desert-savannah ecotone beyond that latitude. Several reasons can explain these differences: For example, the spatial model resolution of the CCM3 simulations was lower, possibly leading to a more crude representation of the atmospheric dynamics during the monsoon season. Model physics, in particular the representation of moist processes, is more elaborate now than more than ten years ago, and this might have led to a stronger and hopefully more realistic sensitivity of the simulated precipitation rates to the presence of open-water surfaces. In addition, synergistic feedbacks between soil albedo and open-water surfaces (via vegetation growth induced by the presence of open-water surfaces) were not taken into account in the previous studies, although this is probably of less importance.

[20] Not only gradual changes of climate forcing parameters, but also climatic extremes on shorter time scales (droughts) potentially induce catastrophic shifts in arid ecosystems when resilience is low [*Scheffer et al.*, 2001]. The analysis of drought occurrences presented above showed that, for a given amount of annual mean precipitation, drought conditions are much less frequent and tend to be less severe in the presence of inland water surfaces. This means that in arid conditions open water surfaces can act as an efficient local moisture source compensating for the lack of long-range atmospheric moisture delivery, thereby reducing the intensity and frequency of dry spells for a given mean annual precipitation rate. In this study, our analysis of drought frequencies and intensities was based on the drought area index defined by *Bhalme and Mooley* [1980]. We carried out analyzes based on alternative indices, such as the number of consecutive dry days [*Frich et al.*, 2002] or the number of years with less than a defined (1/3) fraction of the long-term annual mean precipitation. These alternative analyzes yielded very similar results, increasing our confidence in the results.

[21] The substantial average precipitation increase caused by the mid-Holocene open water surfaces and the reduced drought frequencies and intensities certainly had profound consequences for both the average living conditions and the resource stability for the human populations of the region [*Kuper and Kröpelin*, 2006; *deMenocal*, 2001; *Jousse*, 2006], but a detailed discussion of these consequences is beyond the scope of this paper.

5. Conclusions

[22] Compared to earlier work by *Coe and Bonan* [1997], the present study provides a reassessment of the effect of lakes and wetlands on the North African climate during the mid-Holocene. The open-water surfaces provide often neglected and underestimated feedbacks helping better explain the extent and temporal dynamics of the "Green Sahara". Although the intensity of the effect of open-water surfaces appears to be model-dependent to some degree, this study suggests that taking into account open-water surfaces in studies of similar climatic settings could have beneficial effects.

[23] While stabilizing the Saharan mid-Holocene climate on interannual and intermediate time scales, the inland water surfaces provided a positive feedback on longer (centennial to millennial) time scales which amplified the orbitally induced climate variations at the beginning and the end of the mid-Holocene African humid period, in synergy with other positive feedbacks, and possibly repeatedly since the onset of desert conditions in the Sahara about 7 million years ago [*Schuster et al.*, 2006].

[24] **Acknowledgments.** This research was supported by the Agence Nationale de la Recherche (projects SAHELP and ELPASO [project number 2010 BLANC 608 01]). The authors wish to thank the editor and the reviewers for constructive comments.

[25] The Editor thanks two anonymous reviewers for their assistance in evaluating this paper.

References

Bathiany, S., M. Claussen, and K. Fraedrich (2012), Implications of climate variability for the detection of multiple equilibria and for rapid transitions in the atmosphere-vegetation system, *Clim. Dyn.*, doi:10.1007/s00382-011-1037-x, in press.

Berger, A. (1978), Long-term variations of daily insolation and Quaternary climatic changes, *J. Atmos. Sci.*, *35*, 2362–2367, doi:10.1175/1520-0469(1978)035<2362:LTVODI>2.0.CO;2.

Bhalme, H. N., and D. A. Mooley (1980), Large-scale droughts/floods and monsoon circulation, *Mon. Weather Rev.*, *108*, 1197–1211, doi:10.1175/1520-0493(1980)108<1197:LSDAMC>2.0.CO;2.

Bonfils, C., N. de Noblet-Ducoudré, P. Braconnot, and S. Joussaume (2001), Hot desert albedo and climate change: Mid-Holocene monsoon in North Africa, *J. Clim.*, *14*, 3724–3737, doi:10.1175/1520-0442(2001)014<3724:HDAACC>2.0.CO;2.

Braconnot, P., S. Joussaume, O. Marti, and N. de Noblet (1999), Synergistic feedback from ocean and vegetation on the African monsoon response to mid-Holocene insolation, *Geophys. Res. Lett.*, *26*, 2481–2484, doi:10.1029/1999GL006047.

Braconnot, P., et al. (2007), Results of PMIP2 coupled simulations of the mid-Holocene and Last Glacial Maximum—Part 1: Experiments and large-scale features, *Clim. Past*, *3*, 261–277, doi:10.5194/cp-3-261-2007.

Broström, A., M. Coe, S. P. Harrison, R. Gallimore, J. E. Kutzbach, J. Foley, I. C. Prentice, and P. Behling (1998), Land surface feedbacks and palaeomonsoons in northern Africa, *Geophys. Res. Lett.*, *25*, 3615–3618, doi:10.1029/98GL02804.

Brovkin, V., and M. Claussen (2008), Comment on "Climate-driven ecosystem succession in the Sahara: The past 6000 years," *Science*, *322*, 1326, doi:10.1126/science.1163381.

Charney, J. G. (1975), Dynamics of deserts and drought in Sahel, *Q. J. R. Meteorol. Soc.*, *101*, 193–202, doi:10.1002/qj.49710142802.

Claussen, M., and V. Gayler (1997), The greening of the Sahara during the mid-Holocene: Results of an interactive atmosphere-biome model, *Global Ecol. Biogeogr. Lett.*, *6*, 369–377, doi:10.2307/2997337.

Claussen, M., C. Kubatzki, V. Brovkin, A. Ganopolski, P. Hoelzmann, and H. J. Pachur (1999), Simulation of an abrupt change in Saharan vegetation in the mid-Holocene, *Geophys. Res. Lett.*, *26*, 2037–2040, doi:10.1029/1999GL900494.

Coe, M. T., and G. B. Bonan (1997), Feedbacks between climate and surface water in northern Africa during the middle Holocene, *J. Geophys. Res.*, *102*, 11,087–11,101, doi:10.1029/97JD00343.

Cogley, J. (2003), GGHYDRO—Global Hydrographic Data, release 2.3, *Tech. Note 2003-1*, Dep. of Geogr., Trent Univ., Peterborough, Ont., Canada.

deMenocal, P. B. (2001), Cultural responses to climate change during the last Holocene, *Science*, *292*, 667–673, doi:10.1126/science.1059827.

deMenocal, P. B., J. Ortiz, T. Guilderson, and M. Sarntheim (2000), Coherent high- and low-latitude climate variability during the Holocene warm period, *Science*, *288*, 2198–2202, doi:10.1126/science.288.5474.2198.

Flückiger, J., E. Monnin, B. Stauffer, J. Schwander, T. F. Stocker, J. Chappellaz, D. Raynaud, and J.-M. Barnola (2002), High-resolution Holocene N_2O ice core record and its relationship with CH_4 and CO_2, *Global Biogeochem. Cycles*, *16*(1), 1010, doi:10.1029/2001GB001417.

Frich, P., L. V. Alexander, P. Della-Marta, B. Gleason, M. Haylock, A. M. G. Klein Tank, and T. Peterson (2002), Observed coherent changes in climatic extremes during the second half of the twentieth century, *Clim. Res.*, *19*, 193–212, doi:10.3354/cr019193.

Gasse, F. (2000), Hydrological changes in the African tropics since the Last Glacial Maximum, *Quat. Sci. Rev.*, *19*, 189–211, doi:10.1016/S0277-3791(99)00061-X.

Gasse, F. (2002), Diatom-inferred salinity and carbonate oxygen isotopes in Holocene waterbodies of the western Sahara and Sahel (Africa), *Quat. Sci. Rev.*, *21*, 737–767, doi:10.1016/S0277-3791(01)00125-1.

Hijmans, R. J., S. E. Cameron, J. L. Parra, P. G. Jones, and A. Jarvis (2005), Very high resolution interpolated climate surfaces for global land areas, *Int. J. Climatol.*, *25*, 1965–1978, doi:10.1002/joc.1276.

Hoelzmann, P., D. Jolly, S. P. Harrison, F. Laarif, R. Bonnefille, and H.-J. Pachur (1998), Mid-Holocene land-surface conditions in northern Africa and the Arabian peninsula: A data set for the analysis of biogeophysical feedbacks in the climate system, *Global Biogeochem. Cycles*, *12*, 35–51, doi:10.1029/97GB02733.

Hourdin, F., et al. (2006), The LMDZ4 general circulation model: Climate performance and sensitivity to parametrized physics with emphasis on tropical convection, *Clim. Dyn.*, *27*, 787–813, doi:10.1007/s00382-006-0158-0.

Hulme, M., T. J. Osborn, and T. C. Johns (1998), Precipitation sensitivity to global warming: Comparison of observations with HadCM2 simulations, *Geophys. Res. Lett.*, *25*, 3379–3382, doi:10.1029/98GL02562.

Jousse, H. (2006), What is the impact of Holocene climatic changes on human societies? Analysis of West African Neolithic populations dietary customs, *Quat. Int.*, *151*, 63–73, doi:10.1016/j.quaint.2006.01.015.

Kaplan, J. O., et al. (2003), Climate change and Arctic ecosystems: 2. Modeling, paleodata-model comparisons, and future projections, *J. Geophys. Res.*, *108*(D19), 8171, doi:10.1029/2002JD002559.

Keyantash, J., and J. A. Dracup (2002), The quantification of drought: An evaluation of drought indices, *Bull. Am. Meteorol. Soc.*, *83*, 1167–1180.

Knorr, W., and K.-G. Schnitzler (2006), Enhanced albedo feedback in North Africa from possible combined vegetation and soil-formation processes, *Clim. Dyn.*, *26*, 55–63, doi:10.1007/s00382-005-0073-9.

Krinner, G. (2003), Impact of lakes and wetlands on boreal climate, *J. Geophys. Res.*, *108*(D16), 4520, doi:10.1029/2002JD002597.

Krinner, G., N. Viovy, N. de Noblet-Ducoudre, J. Ogee, J. Polcher, P. Friedlingstein, P. Ciais, S. Sitch, and I. C. Prentice (2005), A dynamic global vegetation model for studies of the coupled atmosphere-biosphere system, *Global Biogeochem. Cycles*, *19*, GB1015, doi:10.1029/2003GB002199.

Kröpelin, S., et al. (2008), Climate-driven ecosystem succession in the Sahara: The past 6000 years, *Science*, *320*, 765–768, doi:10.1126/science.1154913.

Kuper, R., and S. Kröpelin (2006), Climate-controlled Holocene occupation in the Sahara: Motor of Africa's evolution, *Science*, *313*, 803–807, doi:10.1126/science.1130989.

Kutzbach, J. E. (1981), Monsoon climate of the early Holocene: Climate experiment with the Earth's orbital parameters for 9000 years ago, *Science*, *214*, 59–61, doi:10.1126/science.214.4516.59.

Kutzbach, J. E., and Z. Liu (1997), Response of the African monsoon to orbital forcing and ocean feedbacks in the middle Holocene, *Science*, *278*, 440–443, doi:10.1126/science.278.5337.440.

Kutzbach, J. E., G. Bonan, J. Foley, and S. P. Harrison (1996), Vegetation and soil feedbacks on the response of the African monsoon to orbital forcing in the early to middle Holocene, *Nature*, *384*, 623–626, doi:10.1038/384623a0.

Leblanc, M., G. Favreau, J. Maley, Y. Nazoumou, C. Leduc, F. Stagnitti, P. J. van Oevelen, F. Delclaux, and J. Lemoalle (2006), Reconstruction of megalake Chad using Shuttle Radar Topographic Mission data, *Palaeogeogr. Palaeoclimatol. Palaeoecol.*, *239*, 16–27, doi:10.1016/j.palaeo.2006.01.003.

Lézine, A. M. (1989), Late Quaternary vegetation and climate of the Sahel, *Quat. Res.*, *32*, 317–334, doi:10.1016/0033-5894(89)90098-7.

Lézine, A. M., C. Hely, C. Grenier, P. Braconnot, and G. Krinner (2011), Sahara and Sahel vulnerability to climate changes, lessons from Holocene hydrological data, *Quat. Sci. Rev.*, *30*, 3001–3012, doi:10.1016/j.quascirev.2011.07.006.

Liu, Z., Y. Wang, R. Gallimore, M. Notaro, and I. C. Prentice (2006), On the cause of abrupt vegetation collapse in North Africa during the Holocene: Climate variability vs. vegetation feedback, *Geophys. Res. Lett.*, *33*, L22709, doi:10.1029/2006GL028062.

Liu, Z., et al. (2007), Simulating the transient evolution and abrupt change of Northern Africa atmosphere-ocean-terrestrial ecosystem in the Holocene, *Quat. Sci. Rev.*, *26*, 1818–1837, doi:10.1016/j.quascirev.2007.03.002.

Marzin, C., and P. Braconnot (2009), Variations of Indian and African monsoons induced by insolation changes at 6 and 9.5 kyr BP, *Clim. Dyn.*, *33*, 215–231, doi:10.1007/s00382-009-0538-3.

Pachur, H. J., and P. Hoelzmann (2000), Late Quaternary palaeoecology and palaeoclimates of the eastern Sahara, *J. Afr. Earth Sci.*, *30*, 929–939, doi:10.1016/S0899-5362(00)00061-0.

Prentice, I. C., D. Jolly, and BIOME6000 participants (2000), Mid-Holocene and glacial-maximum vegetation geography of the northern continents and Africa, *J. Biogeogr.*, *27*, 507–519, doi:10.1046/j.1365-2699.2000.00425.x.

Rayner, N. A., D. E. Parker, E. B. Horton, C. K. Folland, L. V. Alexander, D. P. Rowell, E. C. Kent, and A. Kaplan (2003), Global analyses of sea surface temperature, sea ice, and night marine air temperature since the late nineteenth century, *J. Geophys. Res.*, *108*(D14), 4407, doi:10.1029/2002JD002670.

Ritchie, J. C., and C. V. Haynes (1987), Holocene vegetation zonation in the eastern Sahara, *Nature*, *330*, 645–647, doi:10.1038/330645a0.

Ritchie, J. C., C. H. Eyles, and C. V. Haynes (1985), Sediment and pollen evidence for an early to mid-Holocene humid period in the eastern Sahara, *Nature*, *314*, 352–355, doi:10.1038/314352a0.

Rossignol-Strick, M. (1983), African monsoon, an immediate climate response to orbital insolation, *Nature*, *304*, 46–49, doi:10.1038/304046a0.

Scheffer, M., S. Carpenter, J. A. Foley, C. Folke, and B. Walker (2001), Catastrophic shifts in ecosystems, *Nature*, *413*, 591–596, doi:10.1038/35098000.

Schuster, M., P. Duringer, J.-F. Ghienne, P. Vignaud, H. T. Mackaye, A. Likius, and M. Brunet (2006), The age of the Sahara desert, *Science*, *311*, 821, doi:10.1126/science.1120161.

Street, A. F., and A. T. Grove (1976), Environmental and climatic implications of late Quaternary lake-level fluctuations in Africa, *Nature*, *261*, 385–390, doi:10.1038/261385a0.

Vamborg, F. S. E., V. Brovkin, and M. Claussen (2011), The effect of a dynamic background albedo scheme on Sahel/Sahara precipitation during the mid-Holocene, *Clim. Past*, *7*, 117–131, doi:10.5194/cp-7-117-2011.

Watrin, J., et al. (2009), Plant migration and plant communities at the time of the "green Sahara," *C. R. Geosci.*, *341*, 656–670, doi:10.1016/j.crte.2009.06.007.

P. Braconnot, C. Grenier, A.-M. Lézine, G. Ramstein, and P. Sepulchre, LSCE/IPSL, CEA/CNRS/UVSQ, F-91191 Gif sur Yvette, France.

I. Gouttevin and G. Krinner, CNRS/Université Joseph Fourier–Grenoble 1, LGGE, F-38041 Grenoble, France. (krinner@lgge.obs.ujf-grenoble.fr)